Inorganic Chemistry

ARTICLE

pubs.acs.org/IC

Multifunctional Magnetic Materials Obtained by Insertion of Spin-Crossover Fe^{III} Complexes into Chiral 3D Bimetallic Oxalate-Based Ferromagnets

Miguel Clemente-León,*[,†] Eugenio Coronado,*[,†] Maurici López-Jordà,[†] and João C. Waerenborgh[‡]

[†]Instituto de Ciencia Molecular, Universidad de Valencia, Catedrático José Beltrán 2, 46980 Paterna, Spain

[‡]Department of Quimica, ITN/CFMC-UL, P-2686-953 Sacavém, Portugal

Supporting Information

ABSTRACT: The syntheses, structures, and magnetic properties of compounds of formula $[Fe^{III}(5\text{-Clsal}_2\text{-trien})][Mn^{II}Cr^{III}(ox)_3]\cdot 0.5(CH_3NO_2)$ (**1**), $[Fe^{III}(5\text{-Brsal}_2\text{-trien})][Mn^{II}Cr^{III}(ox)_3]$ (**2**), and $[In^{III}(5\text{-Clsal}_2\text{-trien})][Mn^{II}Cr^{III}(ox)_3]$ (**3**) are reported. The structure of the three compounds, which crystallize in the orthorhombic $P2_12_12_1$ chiral space group, presents a 3D chiral anionic network formed by Mn^{II} and Cr^{III} ions linked through oxalate ligands with inserted $[Fe^{III}(5\text{-Clsal}_2\text{-trien})]^+$, $[Fe^{III}(5\text{-Brsal}_2\text{-trien})]^+$, and $[In^{III}(5\text{-Clsal}_2\text{-trien})]^+$ cations. The magnetic properties indicate that the three compounds undergo long-range ferromagnetic ordering at ca. 5 K. On the other hand, the inserted Fe^{III} cations undergo a partial spin crossover in the case of **1** and **2**.

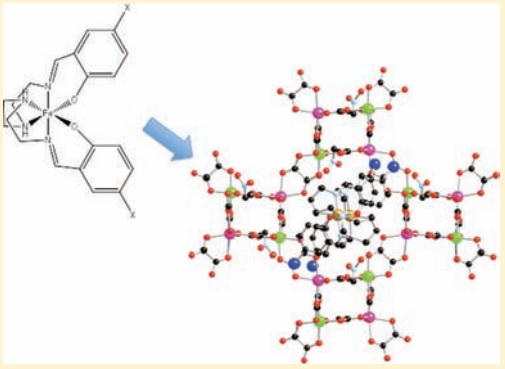

INTRODUCTION

Molecular materials offer great possibilities in the search for novel combinations of properties in a single material. These materials may be prepared building up two network hybrid solids formed by two molecular fragments with each network furnishing distinct physical properties. If the two networks are quasi-independent, a coexistence of the two physical properties is anticipated.[1] If the two molecular networks are coupled, the interplay between their properties may give rise to new properties.[1b] Finally, if one of these two networks changes its properties under application of an external stimulus, a switchable multifunctional material could be obtained in which the responsive network can influence the properties of the other network.[2]

Bimetallic oxalate-bridged complexes of formula $A[M^{II}M^{III}(ox)_3]$ (M^{III} = Cr, Fe, Ru, V, Mn; M^{II} = Mn, Fe, Co, Ni, Cu, Zn; A = cation; ox = oxalate) have provided remarkable examples of this type of compounds.[3] They are composed by polymeric 2D[4] or 3D[5] anionic networks, which furnish the cooperative magnetic properties (ferro-, ferri-, or canted antiferromagnetism), and a bulky charge-compensating molecular cation, which templates the network formation and adds a second physical property to the solid. Insertion of different cations into oxalate networks has led to compounds combining in the same compound the long-range magnetic ordering from the oxalate network with paramagnetism,[6] photochromism,[7] electric conductivity,[8] proton conduction,[9] chirality,[10] chirality and conductivity,[11] or ferroelectricity.[12]

The interplay between the properties of the two molecular networks has been observed in enantiopure oxalate-based magnets prepared by Train et al. that exhibit a magneto-chiral dichroic effect and magnetization-induced second-harmonic generation.[13] Although most of the chiral oxalate-based magnets reported so far present a 3D network and are formed with templating cations that are chiral metallic complexes such as $[Z^{II}(bpy)_3]^{2+}$ (Z = Ru, Fe, Co; bpy = bipyridine) and similar cations,[5,10a,10b] the interplay between chirality and magnetism has only been achieved in enantiopure 2D oxalate-based magnets. A possible explanation to this fact is that the optical properties of the 3D compounds are dominated by absorption of the templating cation.[13a]

The design of switching magnets has been less explored. In this context, cationic spin-crossover (SCO) complexes are particularly suitable for this purpose. This kind of molecular complex changes their spin state from low-spin (LS) to high-spin (HS) configurations under an external stimulus such as temperature, light irradiation, or pressure. As this magnetic switching is accompanied by changes in the molecular size, the spin-crossover process should act as an internal pressure in the hybrid material and therefore might affect the long-range magnetic ordering in the extended magnetic network. In addition, the magnetic framework in which the spin-crossover molecule is inserted may affect the properties of this switchable molecule. Thus far, several examples have described the incorporation of SCO

Received: June 16, 2011
Published: August 16, 2011

Table 1. Crystallographic Data of 1−3

	1	2	3
empirical formula	$C_{26.5}H_{23.5}Cl_2CrFeMnN_{4.5}O_{15}$	$C_{26}H_{22}Br_2CrFeMnN_4O_{14}$	$C_{26}H_{22}Cl_2CrInMnN_4O_{14}$
fw	878.69	937.09	907.14
cryst color	brown	brown	violet
temperature (K)	120	120	120
wavelength (Å)	0.71073	0.71073	0.71073
cryst syst, Z	orthorhombic, 4	orthorhombic, 4	orthorhombic, 4
space group	$P2_12_12_1$	$P2_12_12_1$	$P2_12_12_1$
a (Å)	13.3082(3)	13.6797(11)	13.9216(11)
b (Å)	15.6219(4)	15.2785(9)	15.4812(14)
c (Å)	16.4727(5)	16.0478(13)	15.5450(13)
V (Å^3)	3424.66(16)	3354.1(4)	3350.31(5)
ρ_{calcd} (Mg/m^3)	1.704	1.856	1.798
μ(Mo Kα) (mm^{-1})	1.325	3.570	1.604
θ range (deg)	3.02−32.60	2.87−26.45	2.36−26.48
reflns collected	55 567	15 601	21 374
independent reflns, n (R_{int})	11 701 (0.0616)	6553 (0.066)	6869 (0.152)
L. S. params/restraints	478/1	440/0	436/0
$R1(F)^a I > 2\sigma(I)$]	0.049	0.056	0.073
$wR2(F^2)^b$ all data	0.111	0.108	0.144
$S(F^2)^c$ all data	0.921	1.032	1.006

$^a R1(F) = \Sigma(|F_o| - |F_c|)/\Sigma|F_o|$. $^b wR2(F^2) = [\Sigma w(F_o^2 - F_c^2)^2/\Sigma wF_o^4]^{1/2}$. $^c \Sigma(F^2) = [\Sigma w(F_o^2 - F_c^2)^2/n - p]^{1/2}$.

complexes into oxalate-based networks. While the first ones were solely restricted to Co(II) and Fe(II) complexes,[14] a larger variety of compounds have been recently obtained with Fe(III) complexes of the hexadentate Schiff base ligand, sal$_2$-trien (H_2sal$_2$-trien = *N*,*N*′-disalicylidenetriethylene-tetramine) and derivatives that give rise to 2D and achiral 3D oxalate-based networks.[15,16] The only one showing coexistence of spin crossover and ferromagnetism is the 2D compound [Fe^{III}(sal$_2$-trien)][Mn^{II}Cr^{III}(ox)$_3$]·(CH_2Cl_2) that presents a gradual spin crossover from 350 to 160 K and a ferromagnetic ordering at 5.6 K.[16] Furthermore, it exhibits conversion from the LS to the HS state induced by light irradiation, commonly known as the LIESST effect (light-induced excited spin-state trapping).[17] This is a very rare and unexpected property in a Fe^{III} spin-crossover complex as it has only been found in two other Fe^{III} complexes. Unfortunately, the photoinduced spin conversion of the inserted Fe^{III} complex has a negligible influence on the cooperative magnetic behavior of the oxalate network. This is not unexpected as 2D compounds with different interlayer separation have a very similar Curie temperature (T_c). In this sense, compounds with a 3D network are expected to be better candidates because the T_c of 3D oxalate compounds is very sensitive to the size of the intercalated cation.

In an attempt to insert spin-crossover molecules into a 3D oxalate lattice, we extended this strategy to derivatives of [Fe^{III}(sal$_2$-trien)]$^+$ with Cl and Br substituents on position 5 of the salicylaldimine ring. This resulted in growth of a 3D chiral network in the compounds [Fe^{III}(5-Clsal$_2$-trien)][Mn^{II}Cr^{III}(ox)$_3$]·0.5(CH_3NO_2) (**1**), [Fe^{III}(5-Brsal$_2$-trien)][Mn^{II}Cr^{III}(ox)$_3$] (**2**), and the reference compound [In^{III}(5-Clsal$_2$-trien)][Mn^{II}Cr^{III}-(ox)$_3$]·(CH_3NO_2) (**3**). The structure and magnetic properties of these compounds are reported in this paper.

EXPERIMENTAL SECTION

Complexes [Fe^{III}(5-Clsal$_2$-trien)]PF_6, [Fe^{III}(5-Brsal$_2$-trien)]PF_6, and [In^{III}(5-Clsal$_2$-trien)]PF_6 were prepared according to literature methods.[18] Ag$_3$[Cr(ox)$_3$] was prepared by metathesis from the corresponding potassium salt.[19] All other materials and solvents were commercially available and used without further purification.

[Fe^{III}(5-Clsal$_2$-trien)][Mn^{II}Cr^{III}(ox)$_3$]·0.5(CH_3NO_2) (1), [Fe^{III}-(5-Brsal$_2$-trien)][Mn^{II}Cr^{III}(ox)$_3$] (2), and [In^{III}(5-Clsal$_2$-trien)]-[Mn^{II}Cr^{III}(ox)$_3$]·(CH_3NO_2) (3). Crystals of these compounds were obtained by slow difussion of two solutions. The first solution was prepared by adding $MnCl_2 \cdot 4H_2O$ (0.018 g, 0.09 mmol) to a suspension of $Ag_3Cr(Ox)_3$ (0.038 g, 0.06 mmol) in 3 mL of methanol. The AgCl precipitate was filtered. The second solution was obtained by dissolving [Fe^{III}(5-Clsal$_2$trien)]PF_6 (0.038 g, 0.06 mmol) in 3 mL of nitromethane (**1**), [Fe^{III}(5-Brsal$_2$trien)]PF_6 (0.043 g, 0.06 mmol) in 3 mL of acetonitrile (**2**), or [In^{III}(5-Clsal$_2$trien)]PF_6 (0.042 g, 0.06 mmol) in 3 mL of acetonitrile (**3**). After 2 weeks brown (**1** and **2**) or violet (**3**) crystals were obtained. The composition of these crystals, checked by microanalysis, shows the following M:Mn:Cr:X (M = Fe, In, X = Cl and Br) ratios. Found: 1:1.2:1.1:2 (Fe:Mn:Cr:Cl) for **1**; 1:1.2:1.1:1.9 (Fe:Mn:Cr:Br) for **2**, and 1:1.2:1.1:1.9 (In:Mn:Cr:Cl) for **3**. Calcd: 1:1:1:2 (M:Mn:Cr:X).

Structural Characterization. Single-crystal X-ray data of **1**−**3** were collected at 120 K on a Xcalibur, Sapphire3, Gemini diffractometer equipped with a graphite-monochromated Enhance (Mo) X-ray Source (λ = 0.71073 Å). The program CrysAlisPro, Oxford Diffraction Ltd., Version 1.171.33.52, was used for cell refinements and data reduction of the compounds. Empirical absorption correction was performed using spherical harmonics, implemented in SCALE3 ABSPACK scaling algorithm. Crystal structures were solved by direct methods with the SIR97 program[20] and refined against all F^2 values with the SHELXL-97 program[21] using the WinGX graphical user interface.[22] The three compounds exhibit a Flacks absolute parameter (x) close to 0.[23] This parameter lies within the range that indicates that the absolute structure is valid and that the three crystals are enantiopure. Non-hydrogen atoms were refined anisotropically, and hydrogen atoms were placed in calculated positions refined using idealized geometries (riding model) and assigned fixed isotropic displacement parameters. In **2**, the two terminal ethylene groups from [Fe^{III}(5-Brsal$_2$-trien)]$^+$ complexes were

dx.doi.org/10.1021/ic201293f |*Inorg. Chem.* 2011, 50, 9122–9130

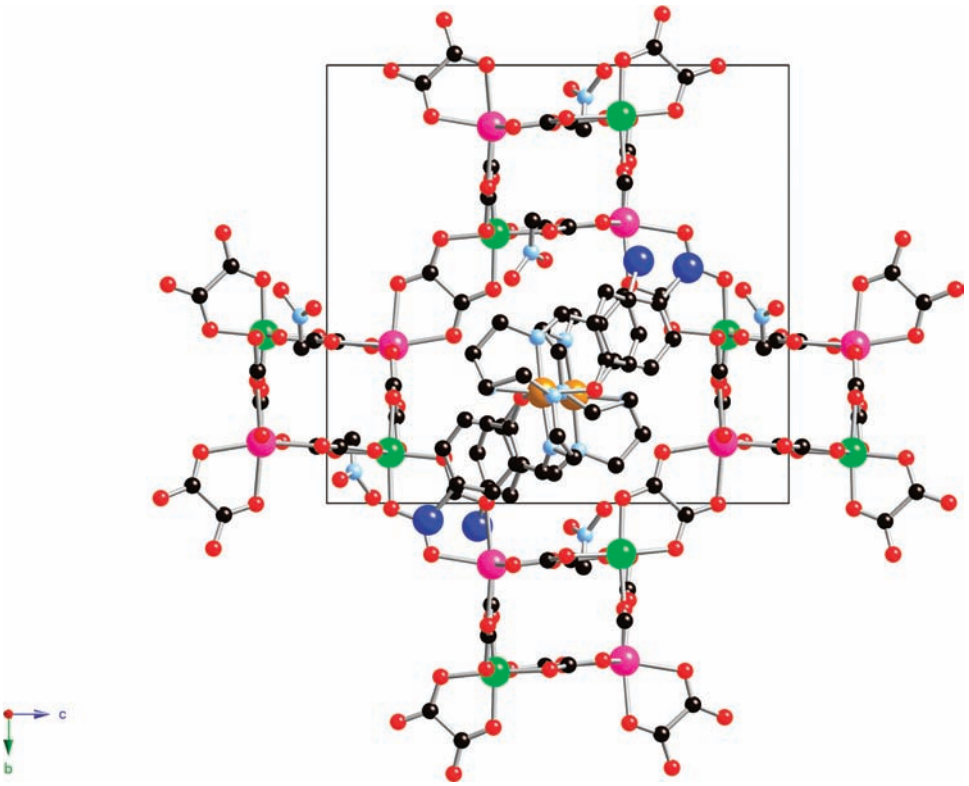

Figure 1. Projection of **1** in the *bc* plane: Fe, yellow; Cr, green; Mn, pink; C, black; N, blue; O, red; Cl, dark blue. Hydrogen atoms have been omitted for clarity.

modeled in two orientations. Data collection and refinement statistics are collected in Table 1.

Physical Measurements. Magnetic susceptibility measurements were performed on polycrystalline samples using a magnetometer (Quantum Design MPMS-XL-5) equipped with a SQUID sensor. Variable-temperature measurements were carried out in the temperature range 2−300 K. The ac measurements were performed in the temperature range 2−10 K at different frequencies with an oscillating magnetic field of 0.395 mT. The magnetization and hysteresis studies were performed between 5 and −5 T, cooling the samples at zero field. The M:Mn:Cr:X (M = Fe, In, X = Cl, Br) ratios were measured on a Philips ESEM X230 scanning electron microscope equipped with an EDAX DX-4 microsonde. Mössbauer spectra were collected in transmission mode using a conventional constant-acceleration spectrometer and a 25 mCi ^{57}Co source in a Rh matrix. The velocity scale was calibrated using α-Fe foil. The absorber was obtained by gently packing single crystals of **1** or **2** into a perspex holder. Low-temperature spectra were collected using a bath cryostat with the sample immersed in liquid He for measurements at 4.1 and 2.2 K or by using flowing He gas to cool the sample above 4.1 K (temperature stability of 0.2 K). The spectra were fitted to Lorentzian lines using a nonlinear least-squares method.[24] Isomer shifts (Tables 2 and 3) are given relative to metallic α-Fe at room temperature.

RESULTS AND DISCUSSION

Synthesis. The method used to prepare $[Fe^{III}(5\text{-}Clsal_2\text{-}trien)][Mn^{II}Cr^{III}(ox)_3]\cdot 0.5(CH_3NO_2)$ (**1**), $[Fe^{III}(5\text{-}Brsal_2\text{-}trien)][Mn^{II}Cr^{III}(ox)_3]$ (**2**), and $[In^{III}(5\text{-}Clsal_2\text{-}trien)][Mn^{II}Cr^{III}(ox)_3]$ (**3**) is similar to that used to prepare the compounds with $[Fe^{III}(sal_2\text{-}trien)]^+$ and the derivatives ($[Fe^{III}(5\text{-}Xsal_2\text{-}trien)]^+$ (X = NO_2 or CH_3O)).[15b,16] It is based on the use of $Ag_3[Cr(ox)_3]$ to avoid the presence of alkali ions in the structure. It consists of slow diffusion of a methanol solution containing the precursors of the oxalate network, Mn^{2+} and $[Cr(ox)_3]^{3-}$ ions, into a solution of $[M^{III}(5\text{-}Xsal_2\text{-}trien)]^+$ (M = Fe or In, X = Cl or Br) in different solvents. In contrast to the compounds with $[Fe^{III}(sal_2\text{-}trien)]^+$ in which the use of different solvents to dissolve the Fe^{III} complex affords compounds with different types of oxalate network (2D for dichloromethane and 3D for acetonitrile), only one type of oxalate network, a chiral 3D network, is obtained for $[Fe^{III}(5\text{-}Xsal_2\text{-}trien)]^+$ (X = Cl or Br) in different solvents. The solvent that leads to the best crystals for X-ray single-crystal diffraction is CH_3NO_2 for $[Fe^{III}(5\text{-}Clsal_2\text{-}trien)]^+$, CH_3CN for $[Fe^{III}(5\text{-}Brsal_2\text{-}trien)]^+$, and CH_3CN for $[In^{III}(5\text{-}Clsal_2\text{-}trien)]^+$ cations.[25] The composition of these crystals, checked by microanalysis, shows in all cases a M:Mn:Cr:X (M = Fe, In, X = Cl and Br) ratio of 1:1:1:2. The crystal structures of the three compounds have been solved by single-crystal X-ray diffraction. Attempts to obtain analogous compounds with other paramagnetic M^{2+} ions (M = Ni, Fe, Co, and Cu) in place of Mn^{2+} have been unsuccessful.

Structure. 1−**3** crystallize in the chiral space group $P2_12_12_1$. As a racemic mixture of $[Cr(ox)_3]^{3-}$ and $[M^{III}(5\text{-}Xsal_2\text{-}trien)]^+$ ions has been used in the synthesis, crystals of both chiralities are obtained as expected.

The structure of **1** is formed by an anionic 3D polymeric oxalate-bridged bimetallic network with $[Fe^{III}(5\text{-}Clsal_2\text{-}trien)]^+$ cations and nitromethane molecules occupying the cavities. This anionic polymeric structure has the well-known 3D 3-connected decagonal oxalate-based anionic network (10,3) which is formed by oxalate ligands connecting Mn^{II} and Cr^{III} ions in such a way that each Mn^{II} is surrounded by three Cr^{III} and vice versa with all metal ions presenting the same chirality (Δ in the crystal used to

dx.doi.org/10.1021/ic201293f |*Inorg. Chem.* 2011, 50, 9122–9130

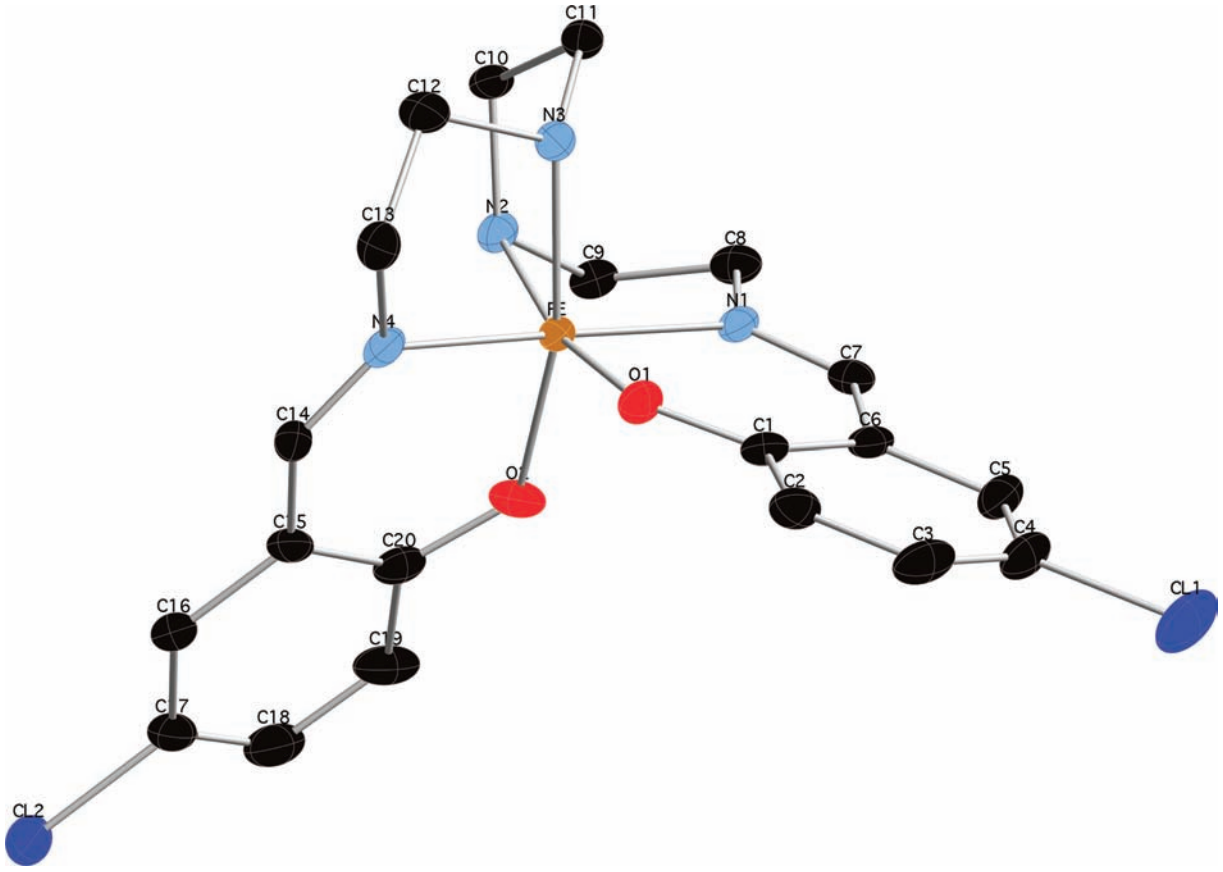

Figure 2. Structural view of $[Fe^{III}(5\text{-}Clsal_2\text{-}trien)]^+$ cation in compound **1**: Fe, yellow; C, black; N, blue; O, red; Cl, dark blue. Hydrogen atoms have been omitted for clarity.

solve the structure). The 3D oxalate chiral network of this compound has some differences with those obtained with $[Z^{II}(bpy)_3]^{2+}$ templating cations. Whereas cations with D_3 symmetry lead to cubic networks, the $[Fe^{III}(5\text{-}Clsal_2\text{-}trien)]^+$ cation gives rise to an orthorhombic network. The consequence of this lower symmetry is that it is possible to distinguish between Mn and Cr ions in the structure of **1** as they present different M−O bond lengths whereas they are disordered in the 3D compound obtained with $[Z^{II}(bpy)_3]^{2+}$. Thus, the two metals are crystallographically independent with mean Mn−O distances of 2.193(3) Å and Cr−O distances of 1.982(3) Å which are typical Mn^{II}−O and Cr^{III}−O distances. Metal−metal distances between adjacent centers are in the range 5.407(6)−5.462(6) Å. These metal−metal distances are longer than those exhibited by the 2D and 3D achiral structures obtained with $[Fe^{III}(sal_2\text{-}trien)]^+$ cations[15b,16] but shorter than those exhibited by other 3D oxalate-based chiral compounds. For instance, the Mn−Cr distance in $[Ir(ppy)_2(bpy)][MnCr(ox)_3]\cdot 0.5H_2O$ is 5.503 Å.[5f] Another consequence of the lower symmetry of the oxalate network is that the projections in the *ab*, *bc*, and *ac* planes are not completely equivalent. The bimetallic oxalate network of **1** defines channels that run along the *a*, *b*, and *c* axis. In contrast with the 3D cubic lattice, in the orthorhombic one the channels running along the *a* axis (Figure 1) present a square shape while those running along the *b* (Figure 1SS, Supporting Information) and *c* axes (Figure 2SS, Supporting Information) are clearly elongated.

The $[Fe^{III}(5\text{-}Clsal_2\text{-}trien)]^+$ complexes and nitromethane molecules are enclosed in the holes described by this 3D oxalate network. There is one crystallographically independent $[Fe(5\text{-}Clsal_2\text{-}trien)]^+$ complex (Figure 2) and disordered nitromethane molecules. In the crystal used to solve the structure, Fe^{III} adopts a Λ configuration, which is the opposite to that shown by Mn^{II} and Cr^{III} ions in the chiral oxalate network. It seems that in contrast to $[Z^{II}(bpy)_3]^{2+}$ cations, $[Fe(5\text{-}Clsal_2\text{-}trien)]^+$ cations induce crystallization of a 3D bimetallic oxalate-based network of opposite chirality. A similar behavior has been observed for another $[Fe(sal_2\text{-}trien)]^+$ derivative ($[Fe(5\text{-}NO_2sal_2\text{-}trien)]^+$), which induces crystallization of a chiral 2D oxalate-based network in which all Cr^{III} centers and $[Fe(5\text{-}NO_2sal_2\text{-}trien)]^+$ presenting short intermolecular contacts are in the opposite configuration.[15b] It is also interesting to observe that $[Fe(5\text{-}Clsal_2\text{-}trien)]^+$ cations form chains that run along the *a* axis within the channels defined by the oxalate network (Figure 1). The CH groups from the two phenoxy rings of one $[Fe(5\text{-}Clsal_2\text{-}trien)]^+$ cation present numerous edge-to-face interactions with CH_2 and NH groups from one of the two neighboring $[Fe(5\text{-}Clsal_2\text{-}trien)]^+$ cations belonging to the same chain. At the same time the CH_2 and NH groups of this $[Fe(5\text{-}Clsal_2\text{-}trien)]^+$ cation are connected through edge-to-face interactions with the two phenoxy rings of the second $[Fe(5\text{-}Clsal_2\text{-}trien)]^+$ neighbor. Furthermore, they present hydrogen bonds through the NH groups with oxalate ligands and numerous short contacts with oxygen atoms from the oxalate network. Finally, the $[Fe(5\text{-}Clsal_2\text{-}trien)]^+$ cations from one chain are connected to the $[Fe(5\text{-}Clsal_2\text{-}trien)]^+$ cations of four neighboring chains through short contacts between Cl atoms and CH_2 from ethylene groups.

dx.doi.org/10.1021/ic201293f |*Inorg. Chem.* 2011, 50, 9122–9130

The nitromethane solvent molecules occupy the holes between the oxalate network and the $[Fe(5\text{-}Clsal_2\text{-}trien)]^+$ cation. They have an ocuppancy of 0.5. CH_3 groups from nitromethane present short contacts with O atoms from the oxalate network, whereas NO_2 groups have short contacts with CH and CH_2 groups from two $[Fe(5\text{-}Clsal_2\text{-}trien)]^+$ complexes belonging to the same chain. The average Fe−N and Fe−O bond distances of $[Fe^{III}(5\text{-}Clsal_2\text{-}trien)]^+$ complexes are 2.009(3) and 1.894(3) Å. These values are intermediate between those obtained for other HS and LS $[Fe(sal_2\text{-}trien)]^+$ compounds. We have to take into account that Mössbauer spectroscopy (see below) indicates that around 70% of Fe is HS at 120 K (temperature at which the crystal structure has been determined).

The structures of **2** and **3** resemble that of **1** with $[Fe^{III}(5\text{-}Brsal_2\text{-}trien)]^+$ or $[In^{III}(5\text{-}Clsal_2\text{-}trien)]^+$ cations in the place of $[Fe^{III}(5\text{-}Clsal_2\text{-}trien)]^+$. The bimetallic oxalate 3D network is similar to that of **1**, but in contrast to **1**, solvent molecules are not found in these two structures. All metal ions from the oxalate network have the same chirality (Λ in the crystals used to solve the structures of **2** and **3**). The two metals are crystallographically independent with mean Mn−O distances of 2.192(5) Å for **2** and 2.186(8) Å for **3** and Cr−O distances of 1.973(5) Å for **2** and 1.973(7) Å for **3**. These distances are again the ones expected for Mn^{II}−O and Cr^{III}−O. Metal−metal distances between adjacent centers are in the range 5.393(5)−5.432(5) Å for **2** and 5.385(7)−5.409(7) Å for **3**.

$[Fe^{III}(5\text{-}Brsal_2\text{-}trien)]^+$ in **2** and $[In^{III}(5\text{-}Clsal_2\text{-}trien)]^+$ in **3** are intercalated in the holes described by the 3D oxalate network. There is one crystallographically independent $[M^{III}(5\text{-}Xsal_2\text{-}trien)]^+$ complex. In the crystals used to solve the structures of **2** and **3**, as for **1**, Fe^{III} and In^{III} adopt the opposite configuration (Δ) to that of Mn^{II} and Cr^{III} ions from the oxalate network (Λ). In **2**, the intermolecular interactions between $[Fe^{III}(5\text{-}Brsal_2\text{-}trien)]^+$ cations are similar to those of **1**. Thus, $[Fe^{III}(5\text{-}Brsal_2\text{-}trien)]^+$ cations ocuppy the channels defined by the oxalate network, forming chains that run along the *a* axis which are connected to the $[Fe^{III}(5\text{-}Brsal_2\text{-}trien)]^+$ cations of four neighboring chains through short contacts between Br atoms and CH_2 from ethylene groups. In **3**, $[In^{III}(5\text{-}Clsal_2\text{-}trien)]^+$ also forms chains but in this case they are only connected through short contacts between Cl atoms and CH_2 from ethylene groups with the $[In^{III}(5\text{-}Clsal_2\text{-}trien)]^+$ of two neighboring chains.

The two ethylene groups closer to the phenoxy rings of $[Fe^{III}(5\text{-}Brsal_2\text{-}trien)]^+$ in **2** are disordered between two possible configurations. The average Fe−N and Fe−O bond distances of $[Fe^{III}(5\text{-}Brsal_2\text{-}trien)]^+$ complexes in **2** are 2.076(7) and 1.913(6) Å. These values are close to those obtained for other HS $[Fe(sal_2\text{-}trien)]^+$ compounds, in agreement with magnetic measurements and Mössbauer spectroscopy (see below), which indicate that around 60% of Fe is HS at 120 K (temperature at which the crystal structure has been determined). The average In−N and In−O bond distances of $[In^{III}(5\text{-}Clsal_2\text{-}trien)]^+$ complexes in **3** are 2.253(8) and 2.114(7) Å.

Magnetic Properties. To get the magnetism of the MnCr oxalate lattice we will talk first of the magnetic properties of **3** as this compound contains a diamagnetic inserted cation. The thermal dependence of the product of the molar magnetic susceptibility times the temperature (χT) of **3** presents a value of 7.0 emu·K·mol^{-1} at 300 K, which is close to the sum of the expected contributions for the isolated paramagnetic ions (see Figure 3). Upon cooling, χT increases gradually with a very abrupt increase below 50 K. This confirms the ferromagnetic

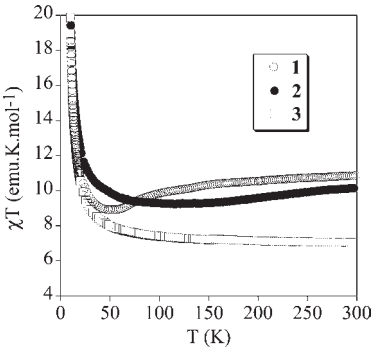

Figure 3. Temperature dependence of the product of the molar magnetic susceptibility with temperature (χT) at 0.1 T for compounds **1** (empty circles), **2** (full circles), and **3** (empty squares).

interaction between Mn^{II} and Cr^{III} ions of the oxalate network and the onset of long-range ferromagnetic ordering, as observed for other Mn^{II}−Cr^{III} oxalate networks.[4−6] The χ^{-1} versus T curve of **3** is linear in the 50−300 K temperature range. This permits one to fit it to a Curie−Weiss law ($\chi^{-1} = (T - \theta)/C$), leading to a Weiss constant, θ (K), of 5.5 K, which is analogous to that obtained for a chiral 3D $Mn^{II}Cr^{III}$ oxalate network in the $[Ir(ppy)_2(bpy)][M^{II}Cr^{III}(ox)_3]\cdot 0.5H_2O$ compound (6.1 K).[5f] To confirm the presence of long-range magnetic ordering and determine precisely the critical temperatures, ac susceptibility measurements were carried out. A maximum in the in-phase signal (χ') near T_c and an out-of-phase signal (χ'') that starts to appear at temperatures just below T_c is observed (Figure 4). From these data the T_c of **3** is 5.0 K. As expected for a ferromagnet, these signals are frequency independent (Figure 4). In the ordered phase an additional peak in χ' and χ'' at temperatures below 3 K is also detected. The presence of such a frequency-dependent peak has already been observed in other 3D bimetallic oxalate compounds.[5f] It can be related with formation of magnetic domains and domain−wall movement in the ordered phase.[26] The isothermal magnetization (M) at 2 K shows a very sharp increase at low fields, reaching a M value of 6.6 μ_B a 0.1 mT (Figure 5), confirming the ferromagnetic interactions between Mn^{II} and Cr^{III} ions. At fields above 0.1 T, only a slight linear increase of M versus H is observed as a consequence of spin canting in the ferromagnetic phase. A M value of 8.0 μ_B is obtained at 5 T, as expected for a $Mn^{II}Cr^{III}$ ferromagnet. A hysteresis loop of the magnetization with a coercive field of 1 mT is observed at 2 K. All these features indicate a ferromagnetic behavior of this 3D oxalate network which is analogous to that obtained in the cubic 3D oxalate-based compounds.[5]

To understand the magnetic properties of **1** and **2** we have to take into account the spin-crossover behavior of the inserted cation besides the ferromagnetic behavior of the MnCr oxalate lattice, mentioned above. χT of **1** and **2** shows higher values than that of **3** in all the range of temperatures due to the paramagnetic contribution of the inserted Fe^{III} cation (see Figure 3). In the case of **1**, it presents a value of 10.9 emu·K·mol^{-1} at 300 K close to the sum of the expected contributions for the isolated paramagnetic ions with the Fe^{III} spin-crossover complex in a HS state. Upon cooling, χT decreases gradually. This decrease is more abrupt below 100 K to reach a minimum of 8.9 emu·K·mol^{-1} around 60 K. This is consistent with a spin crossover of around 50% of Fe^{III} compounds from 300 to 60 K, in agreement with the

dx.doi.org/10.1021/ic201293f |*Inorg. Chem.* 2011, 50, 9122–9130

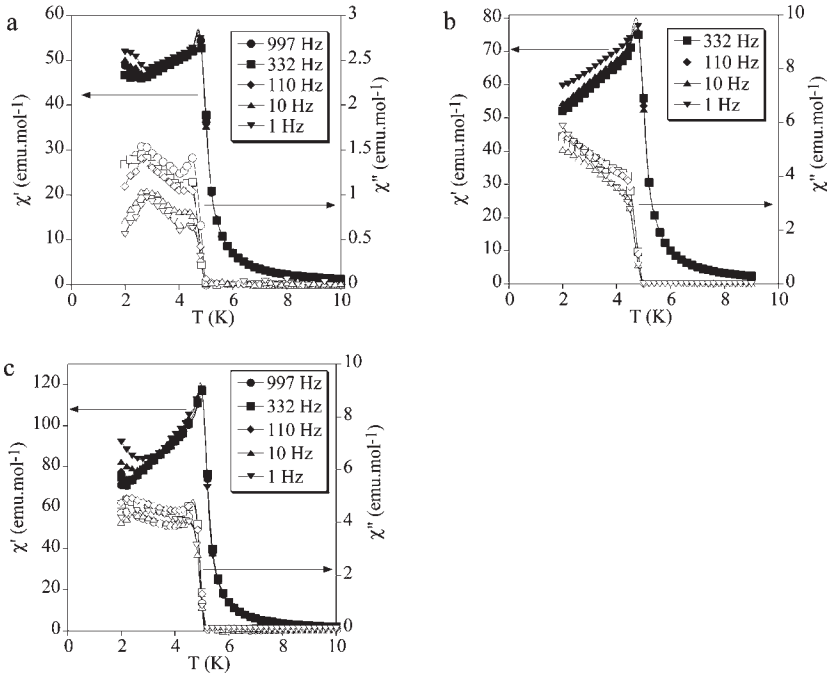

Figure 4. Temperature dependence of the in-phase ac susceptibility (χ') (filled symbols) and out-of-phase ac susceptibility (χ'') of **1** (a), **2** (b), and **3** (c).

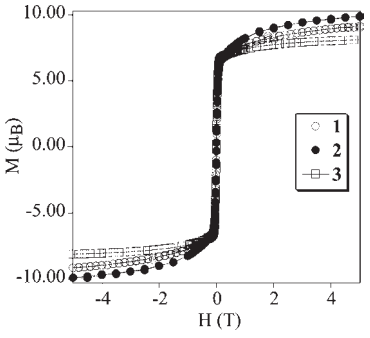

Figure 5. Field dependence of the magnetization (M) for **1** (empty circles), **2** (filled circles), and **3** (empty squares).

data obtained from Mössbauer spectroscopy (see below). χT of **2** is 10.0 emu·K·mol^{-1} at 300 K. This value is slightly lower than that obtained for **1**, in agreement with the 13% of Fe^{III} in the LS state at this temperature calculated from Mössbauer spectroscopy data. At lower temperatures, χT decreases very gradually to reach a minimum of 9.2 emu·K·mol^{-1} around 120 K, in agreement with Mössbauer data that suggest a progressive decrease of the HS fraction between 297 (87% HS) and 100 K (61% HS), which remains constant below this temperature. At temperatures below 80 K, χT of **2** is higher than that of **1** as a result of the smaller degree of HS → LS conversion of **2** (Figure 3). Below 50 K, **1** and **2** present a sharp increase of χT, as in the case of **3**, due to the onset of long-range ferromagnetic ordering.

Alternating current susceptibility measurements of **1** and **2** are very similar to those of **3**. They show frequency-independent peaks in χ' and χ'' and an additional peak in the ordered phase below 3 K (see Figure 4). From these data the T_c of **1** and **2** is 4.8 K. This indicates that the ferromagnetic behavior of the 3D oxalate network of **1** and **2** is analogous to that of **3** with a slight decrease of T_c that may be explained by the shorter $Mn^{II}-Cr^{III}$ distances shown by **3** (5.407(6)−5.462(6) Å for **1**, 5.393(5)−5.432(5) Å for **2**, and 5.385(7) and 5.409(7) Å for **3**) or by slight differences in the bonding angles.

The isothermal magnetization of **1** and **2** at 2 K shows a very sharp increase at low fields, reaching a value of 6.1 μ_B in the two compounds at 0.1 mT, confirming the ferromagnetic interactions between Mn^{II} and Cr^{III} ions. At higher fields M has a continuous increase, which is more important than that of **3** due to the paramagnetic contribution of the inserted Fe^{III} cation. Furthermore, M of the two compounds does not saturate completely (see Figure 5). Due to this, the M value obtained at 5 T (9.1 μ_B) for **1** is still lower than the expected value for a parallel alignement of the spins of Mn^{II} and Cr^{III} with 56% of Fe^{III} in the HS state (11 μ_B) indicated by Mössbauer spectroscopy (see below). This difference may be explained by the spin canting of the bimetallic oxalate network and nonsaturation of the M coming from the paramagnetic Fe^{III} complex. In **2**, the presence of a higher fraction of HS Fe^{III} than that of **1** produces a more pronounced curvature in the M vs H curve that reaches higher M values (Figure 5). Thus, M increases from 6.1 to 9.9 μ_B when H increases from 0.1 to 5 T. Again, this value is lower than the expected one for ∼60% of Fe^{III} in the HS state (∼11.5 μ_B). A hysteresis loop of the magnetization with a coercive field of 3 mT is observed at 2 K for the two compounds.

1−**3** have a slightly lower T_c than that of the cubic 3D chiral compound $[Ir(ppy)_2(bpy)][Mn^{II}Cr^{III}(ox)_3]\cdot 0.5H_2O$ (T_c = 5.1 K)[5f] in spite of the shorter $Mn^{II}-Cr^{III}$ distances that they present. This could be attributed to other factors such as the differences in the relative orientation of the magnetic orbitals. If we compare with other 2D and 3D compounds obtained with $[Fe^{III}(sal_2\text{-trien})]^+$ and derivatives, the T_c value of **1** and **2** (4.8 K) is lower than that exhibited for $Mn^{II}-Cr^{III}$ 2D oxalate (5.6 K) and achiral

dx.doi.org/10.1021/ic201293f |*Inorg. Chem.* 2011, 50, 9122–9130

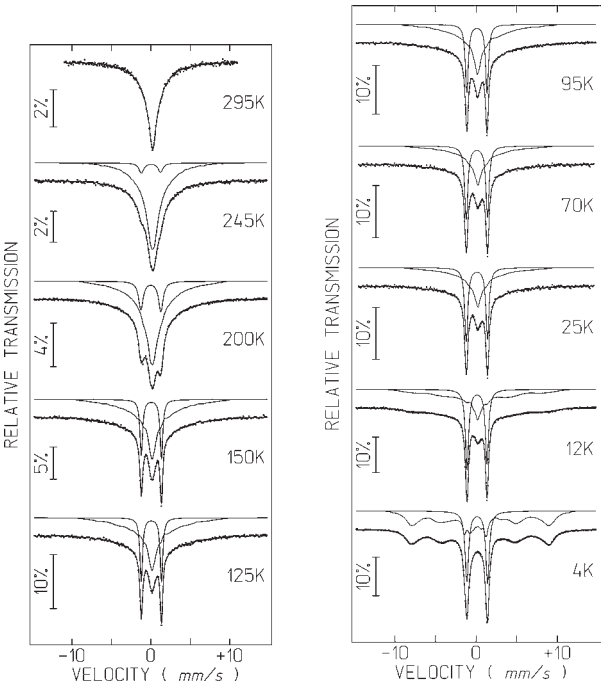

Figure 6. Mössbauer spectra of **1** taken at different temperatures. The lines over the experimental points are the sum of a doublet and a distribution of B_{hf} corresponding to LS and HS Fe^{III}. The estimated parameters for these doublets are collected in Table 2.

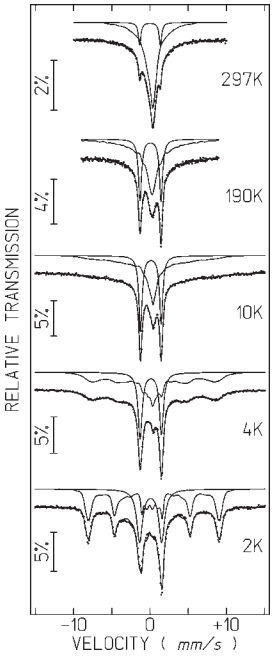

Figure 7. Mössbauer spectra of **2** taken at different temperatures. The lines over the experimental points are the sum of a doublet and a distribution of B_{hf} corresponding to LS and HS Fe^{III}. The estimated parameters for these doublets are collected in Table 3.

3D compounds (5.2 K) with inserted $[Fe^{III}(sal_2\text{-trien})]^+$.[16] This could be explained by the longer $Mn^{II}-Cr^{III}$ distances found in **1** and **2** with respect to these two compounds. Furthermore, we demonstrated that the decrease in T_c observed in the 3D series of

Table 2. Estimated Parameters from the Mössbauer Spectra of 1 Taken at Different Temperatures[a]

T		IS	QS	B_{hf}	I
295 K	LS Fe				
	HS Fe	0.34	0.0		100%
245 K	LS Fe	0.13	2.45		7%
	HS Fe	0.35	0.0		93%
200 K	LS Fe	0.16	2.51		17%
	HS Fe	0.35	0.1		83%
150 K	LS Fe	0.19	2.55		25%
	HS Fe	0.33	0.10		75%
125 K	LS Fe	0.19	2.56		29%
	HS Fe	0.32	0.10		71%
95 K	LS Fe	0.21	2.50		34%
	HS Fe	0.33	0.11		66%
70 K	LS Fe	0.21	2.61		44%
	HS Fe	0.35	0.10		56%
25 K	LS Fe	0.22	2.51		44%
	HS Fe	0.35	0.10		56%
12 K	LS Fe	0.22	2.47		43%
	HS Fe	0.35	0.09		57%
4 K	LS Fe	0.23	2.51		44%
	HS Fe	0.35	0.28	52.8	56%

[a] HS Fe and LS Fe: high-spin and low-spin Fe^{III}; IS (mm/s) isomer shift relative to metallic Fe at 295 K. QS (mm/s) quadrupole splitting of doublets; ε (mm/s), quadrupole shift for magnetic sextet; B_{hf} (T) magnetic hyperfine field. I relative area. Estimated standard deviations are <0.02 mm/s for IS, QS, and Γ, <0.5 T for B_{hf}, and <2% for I.

bimetallic oxalates with respect to the 2D ones can be explained by the noncollinear alignment of the chiral axis in the 3D compounds, as they produce differences in the relative orientation of the magnetic orbitals.[27] On the other hand, in a chiral 3D lattice the T_c values should also be lower than those of achiral 3D lattices with inserted $[Fe^{III}(sal_2\text{-trien})]^+$ as observed for **1** and **2**. That is so because an achiral 3D lattice contains both homochiral (similar to those found in chiral 3D structures) and heterochiral (similar to those found in 2D structures) pairs of neighboring magnetic ions.

Mössbauer Spectroscopy. Mössbauer spectra of **1** and **2** shown in Figures 6 and 7 are similar to those published for $[Fe^{III}(sal_2\text{-trien})][Mn^{II}Cr^{III}(ox)_3]\cdot CH_3OH$ between 2.2 and 295 K and are therefore analyzed with a similar model.[16]

For compound **1** only one contribution is observed at 295 K (Figure 6). It is an unresolved absorption centered at IS $\approx$ 0.34 (295 K) to 0.35 (4 K), which gradually broadens as the temperature decreases and is assigned to HS Fe^{III}. A quadrupole doublet with estimated parameters typical of LS Fe^{III} appears in the 245 K spectrum. The relative area of the quadrupole doublet and therefore the fraction of Fe^{III} in the LS state gradually increases with decreasing temperature down to 100 K. Below 100 K the increase of the LS fraction seems steeper until it reaches approximately 44% at 70 K and stabilizes down to 4.2 K. At this temperature four peak maxima belonging to a sextet appear on the absorption band with an estimated magnetic hyperfine field of 52.8 T typical of HS Fe^{III} (S = 5/2) (Table 2).

For compound **2** two contributions are clearly observed already at 295 K (Figure 7). One is a LS quadrupole doublet. The other one is an unresolved absorption centered at IS $\approx$ 0.31

dx.doi.org/10.1021/ic201293f |Inorg. Chem. 2011, 50, 9122–9130

Table 3. Estimated Parameters from the Mössbauer Spectra of 2 Taken at Different Temperatures[a]

T		IS	QS, ε	B_{hf}	I
295 K	LS Fe	0.11	2.72		13%
	HS Fe	0.31	−0.29		87%
230 K	LS Fe	0.12	2.74		17%
	HS Fe	0.35	−0.13		83%
190 K	LS Fe	0.17	2.76		34%
	HS Fe	0.37	−0.05		66%
100 K	LS Fe	0.18	2.65		39%
	HS Fe	0.39	−0.11		61%
10 K	LS Fe	0.21	2.71		39%
	HS Fe	0.43	−0.15		61%
4 K	LS Fe	0.21	2.79		37%
	HS Fe	0.50	0.21		63%
2 K	LS Fe	0.19	2.89		38%
	HS Fe	0.49	0.21	53.2	62%

[a] HS Fe and LS Fe: high-spin and low-spin Fe^{III}; IS (mm/s) isomer shift relative to metallic Fe at 295 K. QS (mm/s) quadrupole splitting of doublets; ε (mm/s), quadrupole shift for magnetic sextet; B_{hf} (T) magnetic hyperfine field. I relative area. Estimated standard deviations are <0.02 mm/s for IS, QS, and Γ, <0.5 T for B_{hf}, and <2% for I.

(295 K) to 0.50 (4 K) assigned to HS Fe^{III} which gradually broadens as the temperature decreases. At 4 K four peak maxima belonging to a sextet appear on the absorption band. This sextet becomes quite evident at 2.2 K with an estimated magnetic hyperfine field of 53.2 T typical of HS Fe^{III} (S = 5/2). The fraction of Fe^{III} in the LS state increases with decreasing temperature down to 100 K, slowly between 295 and 230 K, fast between 230 and 190 K and again very slowly between 190 and 100 K, where it reaches a value of approximately 38% (Table 3).

As discussed in detail in a previous paper, broadening of the HS Fe^{III} contribution may not be attributed to slow spin state interconversion since the LS Fe^{III} doublet peaks remain sharp with relatively thin line widths in the whole 300−2 K range.[16] Broadening of the HS Fe^{III} is rather due to slow relaxation of the HS Fe^{III} magnetic moments directions with a frequency (10^7−10^9 s^{-1}) whose reciprocal is on the same order of magnitude as the Mössbauer effect observation time. For both **1** and **2** the relaxation frequency decreases with decreasing temperature, as evidenced by the gradual broadening of the absorption until a sextet is observed at 4 K and below, in an identical way as observed for $[Fe^{III}(sal_2\text{-trien})][Mn^{II}Cr^{III}(ox)_3]\cdot(CH_3OH)$.[16] A similar effect has been observed very recently at 3 K in a Fe^{III} complex with a hexadentate Schiff base ligand.[28]

CONCLUSION

In this work we reported the preparation of three novel compounds (**1**−**3**) formed by insertion of the spin-crossover $[Fe^{III}(5\text{-Clsal}_2\text{-trien})]^+$ and $[Fe^{III}(5\text{-Brsal}_2\text{-trien})]^+$ cations and the reference compound with diamagnetic $[In^{III}(5\text{-Clsal}_2\text{-trien})]^+$ cation into anionic coordination polymers based on bimetallic oxalate complexes. We confirm with this result that the use of different sal_2-trien derivatives is a suitable strategy to obtain a great variety of oxalate networks. Thus, we have seen previously that depending on the substituent, different types of networks can be obtained. Thus, $[Fe^{III}(5\text{-NO}_2\text{sal}_2\text{-trien})]^+$ and $[Fe^{III}(5\text{-CH}_3\text{Osal}_2\text{-trien})]^+$ complexes lead, respectively, to formation of 2D and achiral 3D networks, in contrast with the flexibility of nonsubstituted $[Fe(sal_2\text{-trien})]^+$ cation favoring 2D and achiral 3D networks by changing the preparation conditions. In this work, we extended this work to $[Fe^{III}(5\text{-Xsal}_2\text{-trien})]^+$ (X = Cl, Br) complexes, and this has resulted in the growth of a different type of oxalate-based structure, a 3D chiral network. The different templating effect of these cations could be related to the intermolecular interactions. Thus, in $[Fe^{III}(5\text{-NO}_2\text{sal}_2\text{-trien})]^+$ complex the presence of NO_2 groups favors π−π stacking interactions, and this favors growth of a 2D network, while $[Fe^{III}(5\text{-CH}_3\text{Osal}_2\text{-trien})]^+$ complex, which makes more difficult these interactions due to steric hindrance of the methoxy groups, leads to formation of an achiral 3D network. In the three compounds reported in this paper the presence of smaller substituents (Cl or Br) favors a helical arrangement of the complexes and growth of a 3D chiral network. Furthermore, this result shows that formation of oxalate-based chiral 3D networks is not restricted to templating cations such as $[Z^{II}(bpy)_3]^{2+}$. We must take into account that, in contrast to 2D compounds, which admit a large variety of cations, in the 3D structures reported so far the templating cation might have the appropriate symmetry (D_3), size, and charge. This is the first time in which this type of chiral network is obtained with a cation of lower symmetry.

Besides the structural interest of these compounds, we have shown that the strategy reported in this paper gives rise to an unusual combination of three physical properties in the same compound, chirality, spin crossover, and ferromagnetism in the case of **1** and **2** and two properties, chirality and ferromagnetism, in the case of **3**. From the point of view of the onset of new properties, the combination of chirality and ferromagnetism could give rise to the observation of magneto-chiral dichroic effects. Notice that this effect has been observed in the weakly chiral 2D lattice.[13a] Still, in the strongly chiral 3D lattice this effect could not be studied as the charge transfer bands of the $[Z^{II}(bpy)_3]^{2+}$ counterions caused an intense absorption. For this purpose, compound **3** seems to be more promising since Fe^{III} cations of **1** and **2** have an intense absorption due to charge transfer bands and could dominate the optical properties as occurs in the 3D compounds containing $[Z(bpy)_3]^{2+}$ cations. In this context, **3** could be an ideal candidate to observe this effect due to the lack of absorption of the In^{III} complex.

On the other hand, a very promising possibility that remains to be explored is the tuning of the magnetic ordering of the $Mn^{II}Cr^{III}$ oxalate network by inducing the spin crossover of the cations applying light or pressure. Compounds **1** and **2** could be good candidates for this purpose as 3D oxalate networks are expected to be sensitive to the chemical pressure induced by the inserted cation. However, the possible switching effect induced by the presence of the spin-crossover cation could be limited by the gradual and not complete spin crossover (less than 50%) obtained for these compounds.

ASSOCIATED CONTENT

Supporting Information. Projections of the structure of **1** in the *ac* and *ab* planes and CIF files of the structures of **1**−**3**. This material is available free of charge via the Internet at http://pubs.acs.org.

dx.doi.org/10.1021/ic201293f |*Inorg. Chem.* 2011, 50, 9122–9130

AUTHOR INFORMATION

Corresponding Author

*Phone: (+34) 96 3544415. Fax: (+34) 96 354 3273. E-mail: miguel.clemente@uv.es (M.C.-L.); eugenio.Coronado@uv.es (E.C.).

ACKNOWLEDGMENT

Financial support from the EU (SPINMOL ERC Advanced Grant), the Spanish Ministerio de Ciencia e Innovación with FEDER cofinancing (Project Consolider-Ingenio in Molecular Nanoscience and projects MAT2007-61584 and CTQ-2008-06720), and the Generalitat Valenciana (Prometeo Program) are gratefully acknowledged.

REFERENCES

(1) (a) Coronado, E.; Day, P. *Chem. Rev.* **2004**, *104*, 5419. (b) Coronado, E.; Martí-Gastaldo, C.; Navarro-Moratalla, E.; Ribera, A.; Blundell, S. J.; Baker, P. J. *Nat. Chem.* **2010**, *2*, 1031.

(2) (a) Coronado, E.; Giménez-López, M. C.; Levchenko, G.; Romero, F. M.; García-Baonza, V.; Milner, A.; Paz-Pasternak, M. *J. Am. Chem. Soc.* **2005**, *127*, 4580. (b) Coronado, E.; Giménez-López, M. C.; Korzeniak, T.; Levchenko, G.; Romero, F. M.; Segura, A.; García-Baonza, V.; Cezar, J. C.; De Groot, F. M. F.; Milner, A.; Paz-Pasternak, M. *J. Am. Chem. Soc.* **2008**, *130*, 15519.(c) Ohkoshi, S. I.; Imoto, K.; Tsunobuchi, Y.; Takano, S.; Tokoro, H. *Nat. Chem.* **2011**, DOI: 10.1038/NCHEM.1067

(3) Clemente-León, M.; Coronado, E.; Martí-Gastaldo, C.; Romero, F. M. *Chem. Soc. Rev.* **2011**, *40*, 473.

(4) (a) Tamaki, H.; Zhong, Z. J.; Matsumoto, N.; Kida, S.; Koikawa, M.; Achiwa, N.; Hashimoto, Y.; Okawa, H. *J. Am. Chem. Soc.* **1992**, *114*, 6974. (b) Tamaki, H.; Mitsumi, M.; Nakamura, N.; Matsumoto, N.; Kida, S.; Okawa, H.; Ijima, S. *Chem. Lett.* **1992**, 1975. (c) Mathonière, C.; Carling, S. G.; Yuscheng, D.; Day, P. *J. Chem. Soc., Chem. Commun.* **1994**, 1551. (d) Mathonière, C.; Nutall, J.; Carling, S. G.; Day, P. *Inorg. Chem.* **1996**, *35*, 1201. (e) Pellaux, R.; Schmalle, H. W.; Huber, R.; Fisher, P.; Hauss, T.; Ouladdiaf, B.; Decurtins, S. *Inorg. Chem.* **1997**, *36*, 2301. (f) Coronado, E.; Galán-Mascarós, J. R.; Gómez-García, C. J.; Martínez-Agudo, J. M.; Martínez-Ferrero, E.; Waerenborgh, J. C.; Almeida, M. *J. Solid State Chem.* **2001**, *159*, 391. (g) Min, K. S; Rhinegold, A. L.; Miller, J. S. *Inorg. Chem.* **2005**, *44*, 8433. (h) Coronado, E.; Galán-Mascarós, J. R.; Martí-Gastaldo, C. *J. Mater. Chem.* **2006**, *16*, 2685.

(5) (a) Decurtins, S.; Schmalle, H. W.; Schneuwly, P.; Oswald, H. R. *Inorg. Chem.* **1993**, *32*, 1888. (b) Decurtins, S.; Schmalle, H. W.; Schneuwly, P.; Ensling, J.; Gütlich, P. *J. Am. Chem. Soc.* **1994**, *116*, 9521. (c) Hernández-Molina, M.; Lloret, F.; Ruiz-Pérez, C.; Julve, M. *Inorg. Chem.* **1998**, *37*, 4131. (d) Coronado, E.; Galán-Mascarós, J. R.; Gómez-García, C. J.; Martínez-Agudo, J. M. *Inorg. Chem.* **2001**, *40*, 113. (e) Pointillart, F.; Train, C.; Gruselle, M.; Villain, F.; Schmalle, H. W.; Talbot, D.; Gredin, P.; Decurtins, S.; Verdaguer, M. *Chem. Mater.* **2004**, *16*, 832. (f) Clemente-León, M.; Coronado, E.; Gómez-García, C. J.; Soriano-Portillo, A. *Inorg. Chem.* **2006**, *45*, 5653.

(6) (a) Clemente-León, M.; Galán-Mascarós, J. R.; Gómez-García, C. J. *Chem. Commun.* **1997**, 1727. (b) Coronado, E.; Galán-Mascarós, J. R.; Gómez-García, C. J.; Martínez-Agudo, J. M. *Adv. Mater.* **1999**, *11*, 558. (c) Coronado, E.; Galán-Mascarós, J. R.; Gómez-García, C. J.; Ensling, J.; Gutlich *Chem.—Eur. J.* **2000**, *6*, 552.

(7) (a) Bénard, S.; Yu, P.; Audière, J. P.; Rivière, E.; Clèment, R.; Ghilhem, J.; Tchertanov, L.; Nakatami, K. *J. Am. Chem. Soc.* **2000**, *122*, 9444. (b) Aldoshin, S. M.; Sanina, N. A.; Minkin, V. I.; Voloshin, N. A.; Ikorskii, V. N.; Ovcharenko, V. I.; Smirnov, V. A.; Nagaeva, N. K. *J. Mol. Struct.* **2007**, *826*, 69.

(8) (a) Coronado, E.; Galán-Mascarós, J. R.; Gómez-García, C. J.; Laukhin, V. *Nature* **2000**, *408*, 447. (b) Alberola, A.; Coronado, E.; Galán-Mascarós, J. R.; Giménez-Saiz, C.; Gómez-García, C. J. *J. Am. Chem. Soc.* **2003**, *125*, 10774. (c) Coronado, E.; Galán-Mascarós, J. R.; Gómez-García, C. J.; Martínez-Ferrero, E.; Van Smaalen, S. *Inorg. Chem.* **2004**, *43*, 4808.

(9) Okawa, H.; Shigematsu, A.; Sadakiyo, M.; Miyagawa, T.; Yoneda, K.; Ohba, M.; Kitagawa, H. *J. Am. Chem. Soc.* **2009**, *131*, 13516.

(10) (a) Andrés, R.; Gruselle, M.; Malézieux, B.; Verdaguer, M.; Vaissermann, J. *Inorg. Chem.* **1999**, *38*, 4637. (b) Andrés, R.; Brissard, M.; Gruselle, M.; Train, C.; Vaissermann, J.; Malézieux, B.; Jamet, J. P.; Verdaguer, M. *Inorg. Chem.* **2001**, *40*, 4633. (c) Clemente-León, M.; Coronado, E.; Dias, J. C.; Soriano-Portillo, A.; Willett, R. D. *Inorg. Chem.* **2008**, *47*, 6458.

(11) Galán-Mascarós, J. R.; Coronado, E.; Goddard, P. A.; Singleton, J.; Coldea, A. I.; Wallis, J. D.; Coles, S. J.; Alberola, A. *J. Am. Chem. Soc.* **2010**, *132*, 9271.

(12) Endo, T.; Akutagawa, T.; Noro, S. I.; Nakamura, T. *Dalton Trans.* **2011**, *40*, 1491.

(13) (a) Train, C.; Gheorghe, R.; Krstic, V.; Chamoreau, L. M.; Ovanesyan, N. S.; Rikken, G. L. J. A.; Gruselle, M.; Verdaguer, M. *Nat. Mater.* **2008**, *17*, 729. (b) Train, C.; Nuida, T.; Gheorghe, R.; Gruselle, M.; Ohkoshi, S. *J. Am. Chem. Soc.* **2009**, *131*, 16838.

(14) (a) Sieber, R.; Decurtins, S.; Stoeckli-Evans, H.; Wilson, C.; Yufit, D.; Howard, J. A. K.; Capelli, S. C.; Hauser, A. *Chem.—Eur. J.* **2000**, *6*, 361. (b) Coronado, E.; Galán-Mascarós, J. R.; Giménez-López, M. C.; Almeida, M.; Waerenborgh, J. C. *Polyhedron* **2007**, *26*, 1838.

(15) (a) Clemente-León, M.; Coronado, E.; Giménez-López, M. C.; Soriano-Portillo, A.; Waerenborgh, J. C.; Delgado, F. S.; Ruiz-Pérez, C. *Inorg. Chem.* **2008**, *47*, 9111. (b) Clemente-León, M.; Coronado, E.; López-Jordà, M. *Dalton Trans.* **2010**, *39*, 4903.

(16) Clemente-León, M.; Coronado, E.; López-Jordà, M.; Mínguez Espallargas, G.; Soriano-Portillo, A.; Waerenborgh, J. C. *Chem.—Eur. J.* **2010**, *16*, 2207.

(17) Clemente-León, M.; Coronado, E.; López-Jordà, M.; Desplanches, C.; Asthana, S.; Wang, H.; Létard, J.-F. *Chem. Sci.* **2011**, *2*, 1127.

(18) Tweedle, M. F.; Wilson, L. J. *J. Am. Chem. Soc.* **1976**, *98*, 4824.

(19) Baylar, J. C.; Jones, E. M. In *Inorganic Synthesis*; Booth, H. S., Ed.; McGraw-Hill: New York, 1939; Vol. 1, p 35.

(20) Altomare, A.; Burla, M. C.; Camalli, M.; Cascarano, G. L.; Giacovazzo, C.; Guagliardi, A.; Moliterni, A. G. G.; Polidori, G.; Spagna, R. *J. Appl. Crystallogr.* **1999**, *32*, 115.

(21) Sheldrick, G. M. *SHELXL-97*; University of Göttingen: Göttingen, Germany, 1997.

(22) Farrugia, L. J. *J. Appl. Crystallogr.* **1997**, *32*, 837.

(23) Flack, H. D.; Bernardinelli, G. *J. Appl. Crystallogr.* **2000**, *33*, 1143.

(24) Rodrigues, J. V.; Santos, I. C.; Gama, V.; Henriques, R. T.; Waerenborgh, J. C.; Duarte, M. T.; Almeida, M. *J. Chem. Soc., Dalton Trans.* **1994**, 2655.

(25) The use of CH_3NO_2 for $[Fe^{III}(5\text{-Brsal}_2\text{-trien})]^+$ and CH_3CN for $[Fe^{III}(5\text{-Clsal}_2\text{-trien})]^+$ gives rise to crystals with a similar unit cell but lower quality in the case of $[Fe^{III}(5\text{-Brsal}_2\text{-trien})]^+$ and with a high content of impurities in the case of $[Fe^{III}(5\text{-Clsal}_2\text{-trien})]^+$.

(26) Chernova, N. A; Song, Y.; Zavalij, P. Y.; Wittingham, M. S. *Phys. Rev. B* **2004**, *70*, 144405.

(27) Fishman, R. S.; Clemente-León, M.; Coronado, E. *Inorg. Chem.* **2009**, *48*, 3039.

(28) Griffin, M.; Shakespeare, S.; Shepherd, H. J.; Harding, C. J.; Létard, J. F.; Desplanches, C.; Goeta, A. E.; Howard, J. A. K.; Powell, A. K.; Mereacre, V.; Garcia, Y.; Naik, A. D.; Müller-Bunz, H.; Morgan, G. G. *Angew. Chem., Int. Ed.* **2011**, *50*, 896.